Proceedings of ISFOG 2025
5TH INTERNATIONAL SYMPOSIUM ON
FRONTIERS IN OFFSHORE GEOTECHNICS
Nantes, France | June 9-13 2025

ISBN 978-2-85782-758-0

Characterisation of calcareous sediments from the U.S. Southern Atlantic Outer Continental Shelf

B.S. Turner*
The University of Western Australia, Perth, Australia

R. D. Beemer
Virginia Polytechnic Institute and State University, Virginia, United States

M. J. Cabral
The University of Rhode Island, Rhode Island, United States

**benjamin.turner@research.uwa.edu.au*

ABSTRACT: Calcareous sediments of biogenic origin are prevalent throughout the world's low latitude seabed, including the U.S. Southern Atlantic Outer Continental Shelf (OCS) and in the vicinity of offshore wind call areas recently leased through the United States Bureau of Ocean Energy Management. These sediments comprise the skeletal remains of calcium carbonate bearing marine micro- and macro-organisms and their bioclasts, and the grains can vary from hollow round thin-walled foraminifers to bioclasts with highly angular features. Geotechnical design in calcareous sediments is challenging owing to the many uncertainties related to their microscale properties and have been problematic for offshore infrastructure due to the high compressibility and low cyclic strength. To date, no offshore wind developments have been installed in offshore calcareous sediments and it is not yet certain how they will impact the designs of foundations for offshore wind. This study uses non-invasive X-ray micro-computed tomography (µCT) and advanced three-dimensional (3D) image analysis techniques to visually classify and quantify the morphology of calcareous sediments collected during U.S. Government surveys with grab samples off the United States Southern Atlantic coast. The statistics of particle shape parameters and basic index properties of calcareous sediments off the Southern Atlantic OCS are compared to that of previously studied calcareous sediments from Western Australia. The findings presented add to a very limited geotechnical data set of calcareous sediment from the Southern Atlantic OCS and should be helpful for future offshore wind developments in these regions.

Keywords: Calcareous soil; particle shape; micro-scale; x-ray tomography

1 INTRODUCTION

Calcareous sediments comprise of calcium carbonate minerals and are located throughout low latitudinal marine areas (Watson et al. 2019). These sediments of biogenic origin predominately consist of part shells and skeletons of small organisms such as foraminifers, coral, mollusks, and algae (Semple 1988; Coop 1990; Beemer et al. 2018, 2019; Kong and Fonseca 2019).

Geotechnical challenges with calcareous soils include their high compressibility (Valent 1979), low cyclic strength (Mao and Fahey 2003), and low friction angle during compression (Datta et al. 1979; Semple 1988). This can be owed to their crushability which is compounded by hollow particles that release interior voids when crushed (Valent 1979; Beemer et al. 2018). Khorshid (1990) reported the occurrence of pile free-fall, or 'running', during driving of steel pipe piles into calacareous sediments during construction of the North Rankin A natural gas platform on the North West Shelf of Australia. Little resistance was encountered while driving in this area, with pile runs occurring up to 15 meters owing to almost complete loss of interface friction. Mao and Fahey (2003) and Lehane et al. (2014) also demonstrated phase transition behavior among calcareous silts during undrained simple shear and triaxial compression tests, even while containing a greater proportion of sand than clay-sized grains.

Offshore wind has progressed on the East Coast of the United States including off the coast of the Carolinas yet geotechnical research into this region is in its infancy. It was included as a future developement area in Watson et al. (2019) and Zeppilli et al. (2023) investigated sediments from the region off North Carolina, identifying grab samples ranging between 58%-68% carbonate content. The Bureau of Ocean Energy Management on the Atlantic Outer Continental Shelf (Fugro 2022) and the USGS

Atlantic Margin Coring (AMCOR) project (Poppe 1981) have also published studies from the region, varying in distance off the coast of South Carolina and Northern Florida, and extending into the Blake Plateau. The presence of calcareous sediments is likely to be encountered during offshore wind development of the Southeast United States.

Classifying calcareous sediments has traditionally been difficult (Murff 1987; Dutt and Ingram 1990), and while engineering classifications disregard the depositional environment of the sediment, geological classification systems, like Clark and Walker (1977), lack correlation to mechanical properties. Noting that soils with similar material origin and identical particle size distributions can have different mechanical behaviors (Dutt and Ingram 1990), an approach to predict sediment behaviour could be based on their depositional environments of the carbonate ramp, their engineering index properties, and the biological origin of the sediment grains (Beemer et al. 2018). This approach could account for sediments of similar particle size distributions and carbonate contents, assuming for example, that deep-water sediments from low energy environments with large quantities of hollow thin walled foraminifer particles would behave differently than coastal sediments from high energy environments with solid and platy particles. X-ray microtomography imaging is useful for visualizing this difference within soils and help classify them.

2 OFFSHORE CAROLINA CARBONATE SEDIMENTS

The NOAA Index to Marine Lacustrine Geological Samples (National Oceanic and Atmospheric Administration n.d.) has compiled records of offshore cruises from the US Southeast. In this study, samples collected by the *R/V Cape Hatteras* NV 915 and NV 1034 cruises will be profiled for analyses. Three representative grab samples (Fig. 1) from varying depth ranges are presented in Table 1.

Sample 1034-36 was reported to consist of abundant shell fragments, rare quartz, and trace glauconite, dolomite, and coccoliths. Sample 915-27 was reported to consist of abundant shell debris, rare quartz, trace glauconite, sponge spicules, coccoliths, amongst others. 1034-32 was reported to consist of abundant foraminifers, common glauconite, trace shells, sponge spicules, pteropod fragments, amongst others (National Oceanic and Atmospheric Administration n.d.).

Table 1. U.S. Southern Atlantic OCS Calcareous Sediment Properties

Sample	Depth (m)	Location (Lat/Long)	$CaCO_3$ (%)	D_{50} (mm)
1034-36	32	33.87/-77.24	62.40	0.65
915-27	126	33.66/-76.56	86.35	0.59
1034-32	248	33.57/-76.67	68.32	0.32

3 3D X-RAY MICROTOMOGRAPHY AND ANALYSIS

Samples were wet washed through the no. 200 sieve (passing 75µm grains) to remove any salt and fines, then dried in an oven at 50°C. Fines cannot be resolved with these imaging techniques and would impede imaging. XRM was conducted using a Zeiss Xradia versa 610 x-ray microscope operated at 80 kV. A voxel size of 1.5-4.75 µm was used based on the particle size.

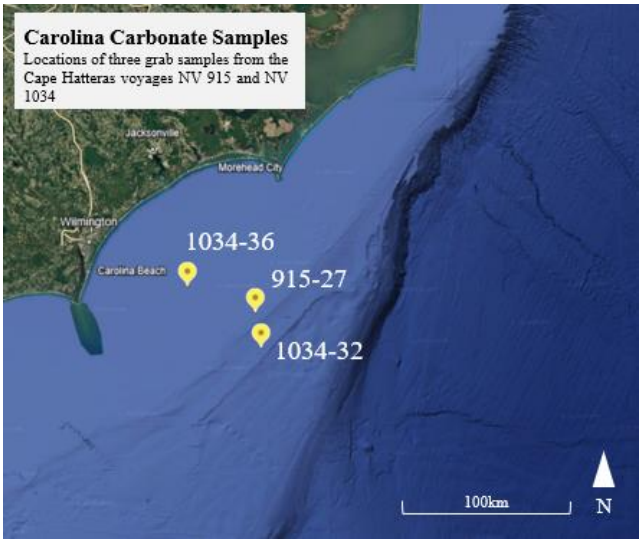

Figure 1. Sample Locations from R/V Cape Hatteras cruises NV 915 and NV 1034 Carolina Carbonate Samples

The µCT images, Fig. 2 (top left), were processed with MATLAB® ver. R2024a. Sample 915-27, 1034-32, and 1034-36 consisted of 1,882, 1,882, and 3,620 slices respectively. Pre-processing was conducted to remove bright spots due to the presence of high-density particles. Pixels with values greater than two standard deviations of the image mean were reduced to the two standard deviations value. The back region outside of the field of view was set to a value similar to the pore volume. Images were segmented with the MATLAB `imsegkmeans3` in sets of 200 slices. Three k-mean clusters were used, one for the background, one for carbonate and glauconite, and a one for silica. The label matrices were then binarized, Fig. 2 (top right). The function `imfill` was applied along each of the three dimensions to fill voids.

A watershed segmentation algorithm was used to separate the individual grains in 3D, Fig. 2 (bottom left). The watershed algorithm was developed by Kong and Fonseca (2018) and improved for computational speed with branch recursive processing by Leonti et al. (2020). The volume was split into four sections along its y-axis and processed in quarters to optimize memory usage. Each section overlapped its neighbor by a third its length to ensure continuity. After segmentation the pixels added during infilling were removed to create the segmented volume, Fig. 2. A masking algorithm was then used to remove edge particles toughing the boundary; most were only partially in the field of view, Fig. 2 (bottom right).

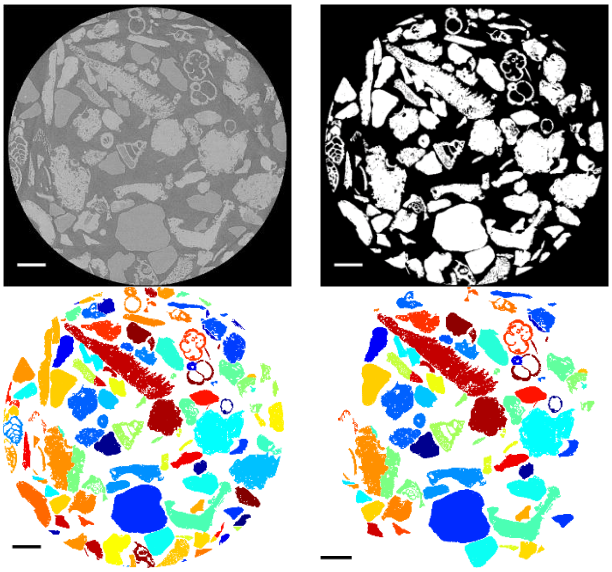

Figure 2. Image processing of Sample 915-27: X-ray microtomography scan prior to binarization (Top Left), Sharpened and threshold image (Top Right), Segmented sample (Bottom Left), Segmented sample with edges removed (Bottom Right). Segmented particles were coloured randomly so individual particles can be more easily identified. White or black bar is 300 µm.

4 3D PARTICLE SHAPE PARAMETERS

The following summarizes the 3D shape parameters used in this study. Feret dimensions ($d_{F\text{-}length}$, $d_{F\text{-}width}$, $d_{F\text{-}thickness}$) where obtained from the principal component analysis in the `regionprops3` function in the previously mentioned software.

Equivalent diameter was calculated as the diameter of a sphere with an equivalent pixel volume:

$$d_{ESD} = \sqrt[3]{\frac{6V}{\pi}}$$

where: d_{ESD} is the equivalent spherical diameter, V is volume of the particle.

Aspect ratio was defined from Zingg (1935) as the ratio of the shortest Feret dimension to the longest.

$$AR = \frac{d_{F-thickness}}{d_{F-length}}$$

where: AR is aspect ratio.

Sphericity was defined from Wadell (1935) as the surface area of a sphere with the same volume as the particle to the surface area of the particle:

$$S = \frac{\pi d_{ESD}^2}{A_s}$$

where: S is sphericity and A_S is the surface area of the particle.

$$C_x = \frac{V}{V_c}$$

where: C_x is convexity, and V_c is the volume of the convex hull of the particle.

5 RESULTS AND DISCUSSION

5.1 µCT Imaging

From visual analysis of the µCT imaging. Fig. 3, the three Carolina calcareous sediments differ in particle shape and type. The foraminifers and shell fragments are apparent in 915-27, Fig. 3 (top right), and 1034-32, Fig. 3 (bottom left). Additionally, glauconite (solid round particles with cracks) can be seen in in 1034-32, Fig. 3 (top right). It can be visually seen particles from closer to the shore, Sample 1034-36, are more angular while particles from offshore, Sample 1034-32, has more hollow particles. Sample 915-27 falls between the two having angular and hollow particles. This is in agreement with R/V Cape Hatteras NV 915 and NV 1034 cruise data and a previous studies in the region Valent (1979) and Zeppilli et al. (2023).

As a comparison, a µCT scan of Ledge Point bioclastic beach sand from Western Australia (Beemer et al. 2022) was provided, Fig. 3 (bottom right). It is visually most similar to 915-27 which was collected from 126 m of water (note scale).

5.2 Particle size distribution

The cumulative particle size distribution (PSD) was calculated from the equivalent spherical diameter, minimum and maximum Feret dimension of

segmented 3D particles. The PSDs from the µCT scans are plotted in comparison to PSD from sieve analysis reported by the research cruise (National Oceanic and Atmospheric Administration n.d.), Fig. 4. The sieve PSD is not provided for 915-27 since it did not meet the requirements of ASTM D6913.

Fig. 4 includes the particle size distribution for the Ledge Point beach sand for comparison. The sieve PSD for the Carolina sediments fell within the Feret range; even with the fines removed prior to scanning. The sieve PSD for the Ledge Point sand fell slightly outside the Feret range, indicating the sand being slightly smaller than what was measured in the µCT analysis, possibly due to sampling differences. The PSDs and D_{50}s of Carolina sediments show that particle size decreases with distance from the coast and water depth, Table 1 and Fig. 4.

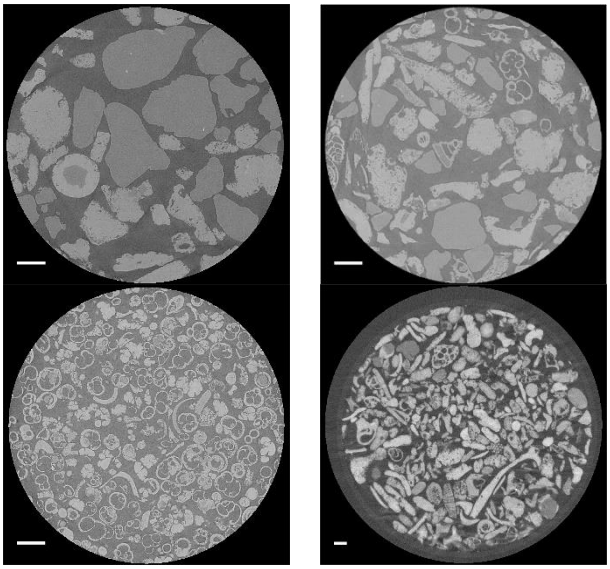

Figure 3. µCT Images of various calcareous sands: 1034-36 water depth = 32 m (top left), 915-27 water depth = 126 m (top right), 1034-32 water depth = 248 m (bottom left), Ledge Point Sand (bottom right), white bar in all images is 300 µm.

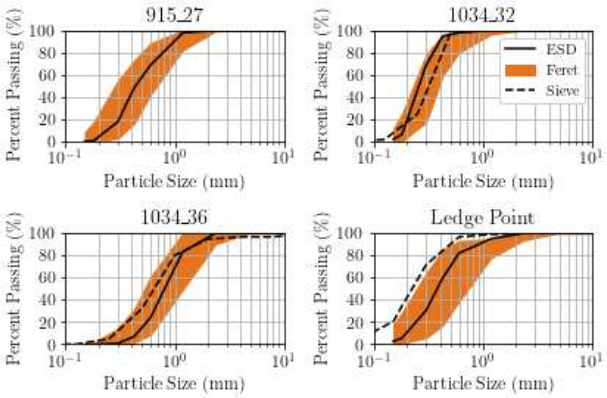

Figure 4. Particle size distributions for samples collected by the R/V Cape Hatteras included in this study, equivalent spherical diameter (ESD) and Feret range

5.3 Statistics of particle shape

Bounded Johnson distributions (Johnson, 1949) fitted to the statistics of Aspect Ratio, Convexity, and Sphericity of the 3D reconstructed and segmented particles are presented for the three Carolina calcareous sediments and the Ledge Point Sand in Fig. 5, using the SciPy distribution fitting function (Virtanen et al 2020). Johnson distributions are used for fitting non-normal geotechnical parameters (Ching and Phoon, 2015). The bounded Johnson distribution is defined by:

$$f(x) = \frac{\delta}{(x-\xi)\left(1-\frac{x-\xi}{\gamma}\right)} \Phi\left(\gamma + \delta \cdot ln\left(\frac{x-\xi}{\lambda+\xi-x}\right)\right)$$

where: Φ is the normal distribution probability density function, x is an independent random variable, δ and γ are fitting parameters, ξ is the location variable, and λ is the scaling variable.

The distributions for the particle shape parameters tend to exhibit similar shapes and skew for all sands except for 1034-32. Aspect ratio, *AR*, skews to the left for aspect ratio, convexity, C_x, skews to the left, and sphericity, *S*, to the right, for all sediments except for 1034-32 which skew in the opposite for *AR* and *S* and has no skew for C_x. As seen in Table 1 and Fig. 3 1034-32 is the sediment with abundant foraminifers and glauconite, while the rest are predominantly bioclastic. Theses difference have a measurable impact on the shape parameters.

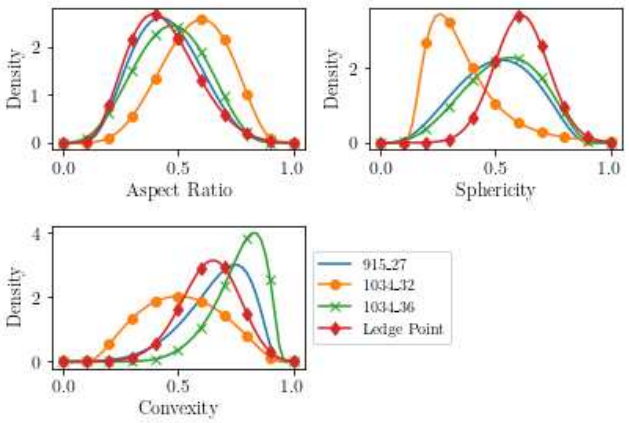

Figure 5. Distribution of 3D Aspect Ratio (Top Left), Convexity (Top Left), and Sphericity (Bottom) of Southern Atlantic OCS Calcareous Sediments

The fitting parameters for the bounded Johnson distribution are provided in Table 2 for all the

sediments. The sphericity parameters for the Ledge Point sand are slightly different than Beemer et al. (2022) due to excluding digital particles smaller than 50 µm created during the shape analysis processes. Shape parameter and Johnson distributions could be useful for reconstructing representative carbonate grains in distinct element and peridynamic models.

5.4 Correlation of particle shape

Coefficients of correlation were calculated for combinations of equivalent spherical diameter, aspect ratio, sphericity, and convexity. Correlations above 0.70 were considered correlated and tabulated in Table 3. Particle size, d_{ESD}, did not correlate with any of the other parameters. The only parameters to show correlation were sphericity, S, and convexity, C_x. This has been seen in other studies on carbonate sediment (Li et al 2021, Beemer et al. 2022, 2024). It is likely a function of intact shells and coral having a relatively high sphericity and convexity and their bioclasts having low ones.

Table 2. Johnson's Bounded Distribution fitting variables to 3D shape parameters

	Aspect Ratio (AR_{3D})	**Convexity (Cx_{3D})**	**Sphericity (S_{3D})**
	915-27 Sand		
γ	5.252e-1	-1.493	-2.316e-1
δ	1.561	1.388	1.286
ξ	3.205e-2	-8.986e-2	-3.163e-3
λ	9.891e-1	1.048	9.415e-1
	1034-32 Sand		
γ	-6.948e-1	8.76e-2	2.893
δ	1.658	1.128	1.424
ξ	-5.636-2	8.515e-2	9.898e-2
λ	1.062	8.907e-1	1.957
	1034-36 Sand		
γ	-9.055e-2	-1.916	-0.3809
δ	1.589	1.370	1.368
ξ	-6.380e-2	-3.134e-2	-4.252e-2
λ	1.039	1.005	9.907e-1
	Ledge Point		
γ	1.358	-4.322	-4.446e6
δ	1.888	4.914	2.198e7
ξ	6.393	-1.492	-5.718e6
λ	1.297	3.020	1.039e7

Table 3. Correlation coefficient of Convexity, C_x, and Sphericity, S, for Calcareous Sediments in this study

915-27	**1034-32**	**1034-36**	**Ledge Point**
0.78	0.84	0.70	0.85

6 CONCLUSIONS

In this study shape parameters from µCT scans were measured from three calcareous sediments from the United States Southern Atlantic OCS and compared to Ledge Point sand from Western Australia. Bounded Johnson Distributions were fitted to measured shape parameters and provided in Table 2. The following conclusions can be drawn.

- The shape parameters of the bioclastic sediment closer to shore, 915-27 and 1034-36, were the most like the Ledge Point beach sand. With 915-27 being the closest, Fig. 5.
- The three sediments varied significantly even though they were from the same region within 65km. Near to shore 1034-36, water depth of 32 m contained quartz and carbonate grains, 915-27, water depth of 126 m was similar, but had more hollow carbonate grains, and 1034-32 contains glauconite and large quantities of hollow foraminifer, Table 1 and Fig. 3.
- Particle size decreases with water depth due to heavier particles being retained in shallow areas nearshore, and lighter particles being transported to offshore, Table 1 and Fig. 4.
- Sphericity and convexity are correlated for these calcareous sediments. This could be due to intact shells having high sphericity and convexity and their bioclasts having low ones.

AUTHOR CONTRIBUTION STATEMENT

B.S. Turner: Data curation, Formal analysis, Writing. **R.D. Beemer**: Software, Conceptualization, Writing. **M.J. Cabral**: X-Ray Mincrotomography, Investigation, Writing.

ACKNOWLEDGEMENTS

The authors wish to thank the Lamont-Doherty Core Repository of Columbia University for samples collected by the R/V Cape Hatteras on Voyages NV 915 and NV 1034. The authors also acknowledge the Australian-American Fulbright Commission for award of the Fulbright Future Scholarship and support of this project.

REFERENCES

Beemer, R., Fonseca, J. and Shaw, J., (2024). Non-invasive characterization of particle morphology of calcareous sands from São Tomé & Príncipe. In E3S Web of Conferences (Vol. 544, p. 04005). EDP Sciences.

Beemer, R. D., Li, L., Leonti, A., Shaw, J., Fonseca, J., Valova, I., Iskander, M., et al. (2022). "Comparison of 2D Optical Imaging and 3D Microtomography Shape Measurements of a Coastal Bioclastic Calcareous Sand." J. Imaging, 8 (3): 20.

Beemer, R. D., A. N. Bandini-Maeder, J. Shaw, U. Lebrec, and M. J. Cassidy. (2018). "The granular structure of two marine carbonate sediments." Proc OMAE2018. Madrid: ASME.

Beemer, R. D., A. Sadekov, U. Lebrec, J. Shaw, A. Bandini Maeder, and M. J. Cassidy. (2019). "Impact of Biology on Particle Crushing in Offshore Calcareous Sediments." GeoCongress 2019, 640–650. Philadelphia, PA: American Society of Civil Engineers.

Ching, J., Phoon. K.-K., (2015). "Constructing multivariate distributions for soil parameters." Risk Reliab. Geotech. Eng., 3–76. Taylor & Francis Boca Raton, FL.

Clark, A. R., and B. F. Walker. (1977). "A proposed scheme for the classification and nomemclature for use in the engineering description on Middle Eastern sedimentary rocks." Géotechnique, 27 (1)

Coop, M. R. (1990). "The mechanics of uncemented carbonate sands." Géotechnique, 40 (4): 607–626.

Datta, M., S. K. Gulhati, and G. V. Rao. (1979). "Crushing Of Calcareous Sands During Shear." Offshore Technology Conference. Houston, Texas: Offshore Technology Conference.

Dutt, R. N., and W. B. Ingram. (1990). "Classification of Marine Sediments." J. Geotech. Engrg., 116 (8): 1288–1289.

Fugro USA Marine Inc. (2022). "Geological and Geotechnical Overview of the Atlantic and Gulf of Mexico Outer Continental Shelf." Desktop study final report commissioned by the Bureau of Ocean Energy Management, Office of Renewable Energy.

Johnson, N. L. (1949). "Systems of Frequency Curves Generated by Methods of Translation." Biometrika, 36 (1/2)

Khorshid, M. S. E. D. (1990). "Development of geotechnical experience on the north west shelf." Trans. Inst. Eng., Aust., Civ. eng, 32 (4): 167–177. Canberra: Institution of Engineers.

Kong, D. & Fonseca, J. (2019). On the kinematics of shelly carbonate sand using X-ray micro tomography. Engineering Geology, 261, 105268.

Lehane, B. M., J. A. H. Carraro, N. Boukpeti, and S. Elkhatib. (2014). "Mechanical Response of Two Carbonate Sediments From Australia's North West Shelf." Volume 3: Offshore Geotechnics, V003T10A008. San Francisco, California, USA: American Society of Mechanical Engineers.

Leonti, A., Fonseca, J., Valova, I., Beemer, R., Cannistraro, D., Pilskaln, C., DeFlorio, D. and Kelly, G., (2020). Optimized 3D segmentation algorithm for shelly sand images. In Proceedings of the 6th World Congress on Electrical Engineering and Computer Systems and Science. Avestia Publishing.

Li, L., R. D. Beemer, and M. Iskander. (2021). "Granulometry of Two Marine Calcareous Sands." J. Geotech. Geoenvironmental Eng., 147 (3)

Mao, X., and M. Fahey. (2003). "Behaviour of calcareous soils in undrained cyclic simple shear." Geotechnique, 53 (8): 715– 727.

Murff, J. D. (1987). "Pile Capacity in Calcareous Sands: State of the Art." J. Geotech. Engrg., 113 (5):490–507

National Oceanic and Atmospheric Administration. n.d. "Index to Marine and Lacustrine Geological Samples doi:10.7289/V5H41PB8." U.S. Department of Commerce. Accessed October 7, 2023.https://www.ngdc.noaa.gov/mgg/curator/curator.html.

Poppe, L. (1981). The 1976 Atlantic Margin Coring (AMCOR) Project. U.S. Geological Survey Open-File Report. United States Geological Survey, Reston, VA.

Semple, R. M. (1988). "Mechanical properties of carbonate soils." Eng. Calcareous Sediments, R. J. Jewell and D. C. Andrews, eds., 807–836. Perth: Balkema.

Valent, P. (1979). "Behavior of two deep ocean calcaresous sediments, including the influence on the performance of the propellant driven anchor." PhD. Purdue University

Virtanen, P., R. Gommers, T. E. Oliphant, M. Haberland, T. Reddy, D. Cournapeau, E. Burovski, et al. (2020). "SciPy 1.0: Fundamental Algorithms for Scientific Computing in Python." Nat. Methods, 17: 261–272.

Watson, P., F. Bransby, Z. L. Delimi, C. Erbrich, I. Finnie, H. Krisdani, C. Meecham, M. et al. (2019). "Foundation Design in Offshore Carbonate Sediments – Building on Knowledge to Address Future Challenges." XVI Pan-Am. Conf. Soil Mech. Geotech. Eng. XVI PCSMGE Res. Appl. Geotech., 35. Cancun, Mexico.

Wadell, H., (1935). "Volume, shape, and roundness of quartz particles." J. Geol., 43 (3): 250–280. University of Chicago Press.

Zeppilli, D., Beemer, R., Turner, B., and Westgate, Z. (2023). "Invoking Carbonate Ramp Theory for Insights into U.S. South-Atlantic Margin Carbonate Sediment Behavior." Volume 1: Proceedings of the 9th International Offshore Site

Investigation and Geotechnics Conference. London, England.
Zingg, T., (1935). "Beitrag zur Schotteranalyse." PhD Thesis. ETH Zurich (in German).